NJC

ROYAL SOCIETY OF CHEMISTRY

PAPER

View Article Online
View Journal | View Issue

Check for updates

Cite this: *New J. Chem.*, 2021, 45, 9501

Immobilized $Zn(OAc)_2$ on bipyridine-based periodic mesoporous organosilica for *N*-formylation of amines with CO_2 and hydrosilanes†

Xiao-Tao Lin,[ab] Kazuhiro Matsumoto,[a] Yoshifumi Maegawa,[c] Katsuhiko Takeuchi,[a] Norihisa Fukaya,[a] Kazuhiko Sato,[a] Shinji Inagaki *[ac] and Jun-Chul Choi *[ab]

Received 12th March 2021,
Accepted 3rd May 2021

DOI: 10.1039/d1nj01204e

rsc.li/njc

Zinc acetate ($Zn(OAc)_2$) was successfully immobilized on a bipyridine-based periodic mesoporous organosilica (BPy-PMO-TMS), as confirmed by solid-state NMR and energy-dispersive X-ray spectroscopies, X-ray diffractometry, and nitrogen adsorption/desorption isotherm analyses. The immobilized Zn complex, $Zn(OAc)_2$(BPy-PMO-TMS), exhibited good catalytic activity during the *N*-formylations of amines and amides with CO_2 and $PhSiH_3$ to produce the corresponding formamides. $Zn(OAc)_2$(BPy-PMO-TMS) with a lower Zn loading was found to exhibit higher catalytic activity.

Published on 05 May 2021. Downloaded by University of Cambridge on 8/31/2021 10:49:26 PM.

Introduction

Periodic mesoporous organosilica (PMO) containing a 2,2′-bipyridine (BPy) unit in its framework has emerged as an efficient solid support for metal complexes due to its unique pore wall structure.[1,2] Since the 2,2′-bipyridine unit is regularly arranged on the pore surface, 1 : 1 metal complexes of BPy are selectively formed on the wall. Moreover, the large (3.8 nm diameter) pores and large (>600 m^2 g^{-1}) surface area of the material enable substrate molecules to smoothly diffuse in its mesopores. These solid support characteristics are advantageous for the immobilization of metal complexes and their application as heterogeneous catalysts for organic transformations. Consequently, a wide variety of transition-metal complexes, including Mn,[3] Ru,[4] Rh,[5] Re,[6] Ir,[7] Pt,[8] and Au complexes,[9] have been immobilized on BPy-PMO, and these immobilized complexes have been used as heterogeneous catalysts for several transformations. While BPy-PMO has a free silanol group on its organosilicate framework, BPy-PMO-TMS, in which the silanols are capped with trimethylsilyl (TMS) groups, is also available, and $Mo(O)_2Cl(OH)$(BPy-PMO-TMS)[10] and $PtMe_2$(BPy-PMO-TMS)[8b] have recently been developed as effective catalysts for olefin epoxidation and alkyne hydrosilylation, respectively.

On the other hand, formamides, as a class of chemical, are widely employed in industry as solvents and raw materials for the syntheses of pharmaceuticals and agrochemicals. The *N*-formylation of an amine with CO_2 (as the C-1 feedstock) and a hydrosilane (as the reductant) is an attractive route to formamides.[11] Since the discovery of organic base-catalyzed *N*-formylation chemistry by Cantat and co-workers,[12] various organocatalysts and metal-based catalysts have been developed for this reaction.[13] We also recently reported that $Zn(OAc)_2$ effectively catalyzes the *N*-formylation and *N*-methylation of nitrogen nucleophiles, such as amines and amides, in the presence of *N*-donor ligands, typically 1,10-phenanthroline.[14] It is noteworthy that $Zn(OAc)_2$ itself cannot promote the reaction. To further develop this chemistry, herein we report the immobilization of $Zn(OAc)_2$ on BPy-PMO-TMS and its use as a heterogeneous catalyst for the *N*-formylations of nitrogen nucleophiles using CO_2 and hydrosilanes.

Results and discussion

Immobilizing $Zn(OAc)_2$ on BPy-PMO-TMS and characterizing $Zn(OAc)_2$(BPy-PMO-TMS)

$Zn(OAc)_2$ was immobilized on BPy-PMO-TMS by simply mixing $Zn(OAc)_2$ and BPy-PMO-TMS (with an initial Zn/BPy molar ratio of 30/100) in MeOH or THF at 60 °C for 24 h (Scheme 1). $Zn(OAc)_2$(BPy-PMO-TMS) **1** (immobilized in MeOH) and **2** (immobilized in THF) were subsequently collected by filtration.

[a] *National Institute of Advanced Industrial Science and Technology (AIST), Tsukuba Central 5, 1-1-1 Higashi, Tsukuba, Ibaraki 305-8565, Japan. E-mail: junchul.choi@aist.go.jp*
[b] *Graduate School of Pure and Applied Sciences, University of Tsukuba, 1-1-1 Tennodai, Tsukuba, Ibaraki 305-8573, Japan*
[c] *Toyota Central R&D Labs., Inc., Nagakute, Aichi 480-1192, Japan. E-mail: inagaki@mosk.tytlabs.co.jp*

† Electronic supplementary information (ESI) available. See DOI: 10.1039/d1nj01204e

Published on 05 May 2021. Downloaded by University of Cambridge on 8/31/2021 10:49:26 PM.

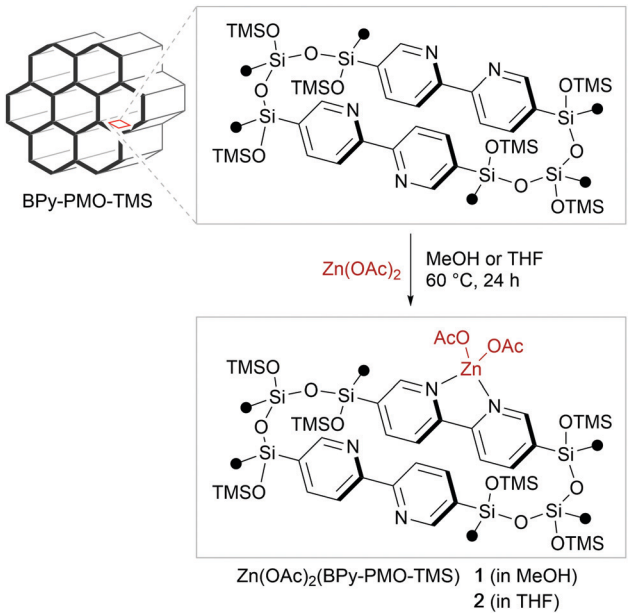

Scheme 1 Immobilization of $Zn(OAc)_2$ on BPy-PMO-TMS.

Comparing the ^{13}C CP/MAS NMR spectra of the parent BPy-PMO-TMS and the immobilized zinc complexes **1** and **2**, with that of the $Zn(OAc)_2$(2,2′-bipyridine)[15] complex clearly reveals that the 2,2′-bipyridine unit of BPy-PMO-TMS is coordinated to $Zn(OAc)_2$ to form the desired $Zn(OAc)_2$(2,2′-bipyridine)-like complexes on the solid support (Fig. 1). The NMR spectra of $Zn(OAc)_2$(BPy-PMO-TMS) **1** and **2** show two new signals corresponding to acetoxy groups at 22 ppm (methyl) and 183 ppm (carbonyl) that are almost identical to those of the $Zn(OAc)_2$(2,2′-bipyridine) complex. However, the spectrum of $Zn(OAc)_2$(BPy-PMO-TMS) **1** immobilized in MeOH reveals a significant decline in the intensity of the peak at around 0 ppm, indicative of partial cleavage of the TMS caps in BPy-PMO-TMS under the immobilization conditions, and TMSOMe was detected by GC/MS and ^1H NMR analysis of the filtrate. On the other hand, no notable decrease in peak intensity was observed in the spectrum of $Zn(OAc)_2$(BPy-PMO-TMS) **2** immobilized in THF. These results indicate that a protonolysis of the O–TMS bonds occurred in protic MeOH.

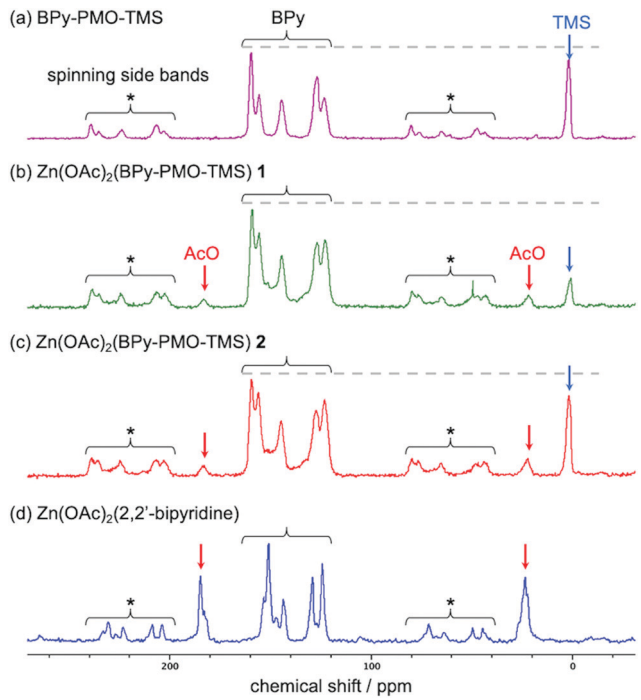

Fig. 1 ^{13}C CP/MAS NMR spectra of (a) BPy-PMO-TMS, (b) $Zn(OAc)_2$(BPy-PMO-TMS) **1** immobilized in MeOH, (c) $Zn(OAc)_2$(BPy-PMO-TMS) **2** immobilized in THF, and (d) $Zn(OAc)_2$(2,2′-bipyridine) complex.

In addition to **2**, $Zn(OAc)_2$(BPy-PMO-TMS) **3** and **4** were prepared in THF with initial Zn/BPy molar ratios of 10/100 (**3**) and 5/100 (**4**). The physicochemical properties of **1–4** are listed in Table 1. The combined filtrate and wash recovered from the immobilization process were subjected to EDX, which revealed that almost all of the $Zn(OAc)_2$ was immobilized on BPy-PMO-TMS in THF, with zinc-atom loadings calculated to be 0.79 (**2**), 0.29 (**3**) and 0.15 mmol g^{-1} (**4**), respectively, whereas incomplete immobilization was observed in MeOH (Zn amount of **1**: 0.69 mmol g^{-1}). $Zn(OAc)_2$(BPy-PMO-TMS) **1–4** showed similar type-IV isotherms in nitrogen adsorption/desorption experiments (Fig. S1–S5, ESI†), which indicates that the uniform mesoporosity of the parent BPy-PMO-TMS was maintained in $Zn(OAc)_2$(BPy-PMO-TMS) **1–4**. $Zn(OAc)_2$(BPy-PMO-TMS) **3** was subjected to XRD, which confirmed that the mesoporous structure of BPy-PMO-TMS was maintained during the immobilization process (Fig. S6, ESI†).

Catalytic performance of $Zn(OAc)_2$(BPy-PMO-TMS)

We next investigated the heterogeneous catalytic *N*-formylation of *N*-methylaniline (**5a**) with CO_2 (0.5 MPa) and $PhSiH_3$ (1 mmol) at 60 °C over $Zn(OAc)_2$(BPy-PMO-TMS) **1–4** (Table 2). $Zn(OAc)_2$(BPy-PMO-TMS) **2** immobilized in THF showed slightly higher yield than $Zn(OAc)_2$(BPy-PMO-TMS) **1** immobilized in MeOH (entries 1 and 2). It is noteworthy that catalytic performance is strongly affected by the Zn loading on the solid support. Even in the presence of the same Zn-based catalyst loading (2 mol% Zn), $Zn(OAc)_2$(BPy-PMO-TMS) **3** (0.29 mmol Zn g^{-1}) showed higher catalytic activity than **2** (0.79 mmol Zn g^{-1}) (entries 2 and 3). A similar trend was observed during *N*-formylations using 1 mol%

Table 1 Physicochemical properties of BPy-PMO-TMS and $Zn(OAc)_2$(BPy-PMO-TMS) **2–4**

	Zn amount[a,b] (mmol g^{-1})	S_{BET}[c] (m^2 g^{-1})	d_{DFT}[c] (nm)
BPy-PMO-TMS	—	877	4.4
1	0.69 (30/100)	630	4.6
2	0.79 (30/100)	804	4.1
3	0.29 (10/100)	856	4.3
4	0.15 (5/100)	866	4.4

[a] Calculated from unimmobilized Zn amount. [b] The number in parentheses is an initial Zn/BPy molar ratio. [c] Determined from nitrogen adsorption–desorption isotherms at liquid-nitrogen temperature and calculated using the BET method (S_{BET}) or density functional theory (d_{DFT}).

 This journal is © The Royal Society of Chemistry and the Centre National de la Recherche Scientifique 2021

Published on 05 May 2021. Downloaded by University of Cambridge on 8/31/2021 10:49:26 PM.

Table 2 $Zn(OAc)_2$(BPy-PMO-TMS)-catalyzed *N*-formylations of *N*-methylaniline (**5a**) using CO_2 and phenylsilane

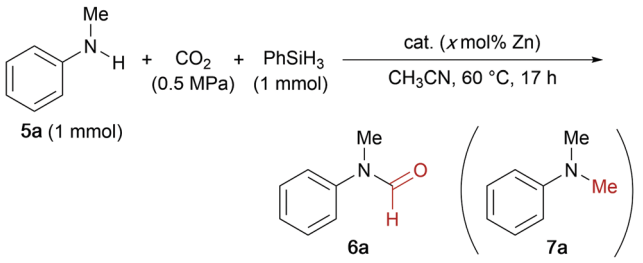

Entry	Cat.	*x* (mol%)	Yield of **6a**[a] (%)	Yield of **7a**[a] (%)
1	**1** (28 mg)	2	39	1
2	**2** (25 mg)	2	43	1
3	**3** (69 mg)	2	94	2
4	**3** (35 mg)	1	86 (80)[b]	2
5	**4** (67 mg)	1	93	2
6	**4** (34 mg)	0.5	78	2
7	BPy-PMO-TMS (69 mg)	—	6	1
8	$Zn(OAc)_2$	1	Trace	Trace
9	$Zn(OAc)_2$(2,2′-bipyridine)	2	97	2

[a] Determined by HPLC analysis. [b] Isolated yield.

Zn: **3** (0.29 mmol Zn g^{-1}) and **4** (0.15 mmol Zn g^{-1}) (entries 4 and 5). Since it is well-known that zinc carboxylates generate oligomeric and polymeric species through carboxylate bridges,[15a,16] $Zn(OAc)_2$(BPy-PMO-TMS) with a higher Zn loading is expected to contain a somewhat higher amount of inactive zinc species that are not coordinated to BPy groups but form acetate-bridged oligomers. The parent BPy-PMO-TMS also provided formamide **6a** under the above mentioned conditions, albeit in only 6% yield (entry 7). In addition, a trace amount of **6a** was detected when $Zn(OAc)_2$ was used as the catalyst (entry 8), and $Zn(OAc)_2$(2,2′-bipyridine) showed high catalytic activity comparable to that of $Zn(OAc)_2$(BPy-PMO-TMS) **3** and **4** (entry 9). These results support the notion that the $Zn(OAc)_2$(2,2′-bipyridine)-like complex on the solid support observed in Fig. 1 is an active *N*-formylation catalyst or precatalyst. While Beller and co-workers reported that $Zn(OAc)_2$ is a good catalyst for the reductions of amides with hydrosilanes,[17] the formation of *N*,*N*-dimethylaniline (**7a**), which is formed by the reduction of *N*-methyl formamide **6a**, was sufficiently suppressed under the reaction conditions.[18]

While $Zn(OAc)_2$(BPy-PMO-TMS) **4** showed better catalytic performance per zinc than **3**, the performance of **4** per unit weight was higher for **3**. Therefore, $Zn(OAc)_2$(BPy-PMO-TMS) **3** was applied for *N*-formylation of various nitrogen nucleophiles **5** (Scheme 2). *N*-Methylaniline derivative **5b**, which bears an electron-donating (MeO–) group on its benzene ring, reacted smoothly to give the corresponding formamide **6b** in 86% yield. A lower (60%) yield of the corresponding formamide **6c** was obtained when *N*-methylaniline derivative **5c**, with an electron-withdrawing (Cl–) group, was used; however, extending the reaction time to 24 h led to an improved yield of 80%. While morpholine (**5d**) and aniline (**5e**) were also good *N*-formylation substrates to give the corresponding formamides **6d** (88%) and **6e** (70%), benzylamine (**5f**) reacted sluggishly under

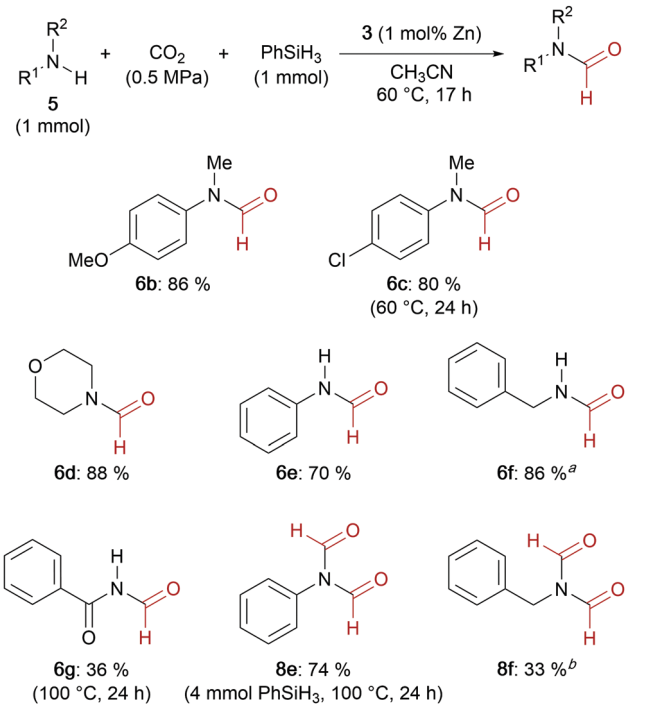

Scheme 2 Substrate scope of $Zn(OAc)_2$(BPy-PMO-TMS)-catalyzed *N*-formylation of nitrogen nucleophiles **5**. [a]After the reaction of $PhSiH_3$ and CO_2 at 60 °C for 17 h, substrate was added and the mixture was stirred at room temperature for 30 min. [b]After the reaction of $PhSiH_3$ (4 mmol) and CO_2 at 60 °C for 17 h, substrate was added and the mixture was stirred at 100 °C for 24 h.

the standard conditions (12% yield). We assume that **5f** coordinates to the zinc center to inhibit the production of silyl formate. Therefore, after the silyl formate from $PhSiH_3$ and CO_2 was generated at 60 °C for 17 h, **5f** was added to the reaction mixture; an 86% yield of **6f** was obtained under these stepwise conditions. Although benzamide (**5g**) was also able to be *N*-formylated, the yield of **6g** was only 36% even at 100 °C due to its low nucleophilicity. Progress during the *N*-formylations of amides reveals that primary amines should be able to be double *N*-formylated. Indeed, the double formylated product **8e** was obtained in 74% yield when aniline was treated with excess $PhSiH_3$ (4 mmol) at 100 °C for 24 h. Benzylamine was two-fold *N*-formylated to give **8f** using the stepwise method with excess $PhSiH_3$ (4 mmol), albeit in a moderate yield of 33%.

Although the detailed mechanism is still unclear, a plausible pathway is illustrated in Scheme 3, based on the previous study of the *N*-formylation using homogeneous $Zn(OAc)_2$/1,10-phenanthroline catalyst.[14] In the presence of $Zn(OAc)_2$(BPy-PMO-TMS), CO_2 reacts with phenylsilane to give the corresponding silyl formates, $PhSiH_{3-n}(OC(=O)H)_n$ (n = 1–3). Amine nucleophiles can attack the silyl formates even in the absence of the Zn catalyst to afford the desired *N*-formylated products with the coproduction of phenylsilanols, $PhSiH_{3-n}(OC(=O)H)_{n-m}(OH)_m$ (n = 1–3, m = 1–3, $n \geq m$). In the reaction of amide nucleophiles, which are less nucleophilic than amines, the Zn catalyst facilitates the *N*-formylation process at higher temperature of 100 °C.

Published on 05 May 2021. Downloaded by University of Cambridge on 8/31/2021 10:49:26 PM.

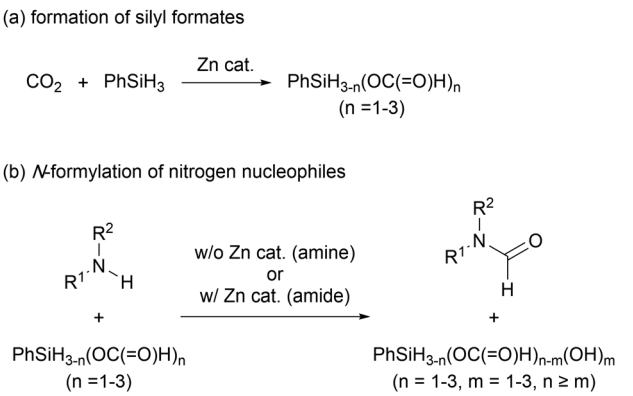

Scheme 3 A plausible pathway to *N*-formylated products: (a) formation of silyl formates from CO_2 and phenylsilane and (b) *N*-formylation of nitrogen nucleophiles with silyl formates.

Analyzing the recovered catalyst

We investigated the recovery and reuse of $Zn(OAc)_2$(BPy-PMO-TMS) **3**. After *N*-methylaniline had been *N*-formylated, the immobilized catalyst was recovered by filtration, washed with CH_3CN, dried *in vacuo*, and used in a second reaction; however, a significantly lower product yield (79%) was observed. The ^{13}C CP/MAS NMR spectrum of the recovered catalyst shows a remarkable decline in intensity of the peak at around 0 ppm and new signals at around 140–120 ppm, indicative of the partial cleavage of the TMS caps of BPy-PMO-TMS and contamination by benzene derivatives (Fig. S7, ESI†). The appearance of a shoulder at around −70 ppm in the ^{29}Si CP/MAS NMR spectrum, which is assigned to the T^2 unit, and a new peak at around −45 ppm, also support a TMS cleavage process and contamination by PhSi$\equiv$ species (Fig. S8, ESI†). Since the *N*-formylation using phenylsilane concomitantly produces the phenylsilanol derivatives (Scheme 3b), we assume that the silanol derivatives cleave the TMS caps through protonolysis to form siloxane bonds through dehydrative condensation with the deprotected silanols of the BPy-PMO framework (Scheme 4). In fact, the nitrogen adsorption/desorption isotherm of the recovered $Zn(OAc)_2$(BPy-PMO-TMS) reveals a significant decrease in adsorbed amount of nitrogen (Fig. S9, ESI†), whereas XRD shows that the ordered mesostructure of the BPy-PMO framework had been preserved (Fig. S6, ESI†). Therefore, we conclude that mesopore occlusion by coproduced silanols is the main factor that prevents catalyst reuse.

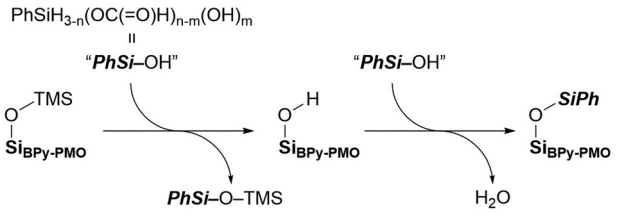

Scheme 4 A possible mechanism for cleavage of TMS cap and incorporation of PhSi$\equiv$ species.

Conclusions

We immobilized a zinc complex on a periodic mesoporous organosilica to form $Zn(OAc)_2$(BPy-PMO-TMS), and used it as a heterogeneous catalyst for the *N*-formylations of nitrogen nucleophiles with CO_2 as the C-1 source and phenylsilane as the reductant. $Zn(OAc)_2$(BPy-PMO-TMS) with a lower Zn loading exhibited higher catalytic performance for the *N*-formylation of *N*-methylaniline. However, the co-production of phenylsilanol derivatives during *N*-formylation led to occlusion of the solid-support mesopores, which prevented catalyst reuse.

Conflicts of interest

There are no conflicts to declare.

Acknowledgements

The authors thank Yuta Hashiguchi for XRD analysis and Dr Yu Shinke and Takahito Sakuraba for nitrogen adsorption/desorption measurements.

Notes and references

1 N. Mizoshita, T. Tani and S. Inagaki, *Chem. Soc. Rev.*, 2011, **40**, 789.
2 M. Waki, Y. Maegawa, K. Hara, Y. Goto, S. Shirai, Y. Yamada, N. Mizoshita, T. Tani, W. Chun, S. Muratsugu, M. Tada, A. Fukuoka and S. Inagaki, *J. Am. Chem. Soc.*, 2014, **136**, 4003.
3 X. Wang, I. Thiel, A. Fedorov, C. Copéret, V. Mougel and M. Fontecave, *Chem. Sci.*, 2017, **8**, 8204.
4 (*a*) M. Waki, S. Shirai, K. Yamanaka, Y. Maegawa and S. Inagaki, *RSC Adv.*, 2020, **10**, 13960; (*b*) Y. Kuramochi, M. Sekine, K. Kitamura, Y. Maegawa, Y. Goto, S. Shirai, S. Inagaki and H. Ishida, *Chem. – Eur. J.*, 2017, **23**, 10301; (*c*) N. Ishito, H. Kobayashi, K. Nakajima, Y. Maegawa, S. Inagaki, K. Hara and A. Fukuoka, *Chem. – Eur. J.*, 2015, **21**, 15564.
5 (*a*) T. Himiyama, M. Waki, Y. Maegawa and S. Inagaki, *Angew. Chem., Int. Ed.*, 2019, **58**, 9150; (*b*) K. Matsui, Y. Maegawa, M. Waki, S. Inagaki and Y. Yamamoto, *Catal. Sci. Technol.*, 2018, **8**, 534.
6 M. Waki, K. Yamanaka, S. Shirai, Y. Maegawa, Y. Goto, Y. Yamada and S. Inagaki, *Chem. – Eur. J.*, 2018, **24**, 3846.
7 (*a*) S. Yamaguchi, Y. Maegawa, N. Onishi, R. Kanega, M. Waki, Y. Himeda and S. Inagaki, *ChemCatChem*, 2019, **11**, 4797; (*b*) X. Liu, Y. Maegawa, Y. Goto, K. Hara and S. Inagaki, *Angew. Chem., Int. Ed.*, 2016, **55**, 7943; (*c*) Y. Maegawa and S. Inagaki, *Dalton Trans.*, 2015, **44**, 13007; (*d*) W. R. Grüning, G. Siddiqi, O. V. Safonova and C. Copéret, *Adv. Synth. Catal.*, 2014, **356**, 673.
8 (*a*) H. Matsukawa, M. Yoshida, T. Tsunenari, S. Nozawa, A. Sato-Tomita, Y. Maegawa, S. Inagaki, A. Kobayashi and M. Kato, *Sci. Rep.*, 2019, **9**, 15151; (*b*) Y. Naganawa, Y. Maegawa, H. Guo, S. S. Gholap, S. Tanaka, K. Sato, S. Inagaki and Y. Nakajima, *Dalton Trans.*, 2019, **48**, 5534.

 This journal is © The Royal Society of Chemistry and the Centre National de la Recherche Scientifique 2021

Published on 05 May 2021. Downloaded by University of Cambridge on 8/31/2021 10:49:26 PM.

9 N. Ishito, K. Nakajima, Y. Maegawa, S. Inagaki and A. Fukuoka, *Catal. Today*, 2017, **298**, 258.
10 S. Ishikawa, Y. Maegawa, M. Waki and S. Inagaki, *ACS Catal.*, 2018, **8**, 4160.
11 (*a*) R. A. Pramudita and K. Motokura, *ChemSusChem*, 2021, **14**, 281; (*b*) S. Dabral and T. Schaub, *Adv. Synth. Catal.*, 2019, **361**, 223; (*c*) H. Seo, L. V. Nguyen and T. F. Jamison, *Adv. Synth. Catal.*, 2019, **361**, 247; (*d*) N. A. Tappe, R. M. Reich, V. D'Elia and F. E. Kühn, *Dalton Trans.*, 2018, **47**, 13281; (*e*) J. Artz, T. E. Müller, K. Thenert, J. Kleinekorte, R. Meys, A. Sternberg, A. Bardow and W. Leitner, *Chem. Rev.*, 2018, **118**, 434; (*f*) Q. Liu, L. Wu, R. Jackstell and M. Beller, *Nat. Commun.*, 2015, **6**, 5933; (*g*) G. Fiorani, W. Guo and A. W. Kleij, *Green Chem.*, 2015, **17**, 1375; (*h*) M. Aresta, A. Dibenedetto and A. Angelini, *Chem. Rev.*, 2014, **114**, 1709; (*i*) C. Maeda, Y. Miyazaki and T. Ema, *Catal. Sci. Technol.*, 2014, **4**, 1482; (*j*) M. Cokoja, C. Bruckmeier, B. Rieger, W. A. Herrmann and F. E. Kühn, *Angew. Chem., Int. Ed.*, 2011, **50**, 8510; (*k*) T. Sakakura, J.-C. Choi and H. Yasuda, *Chem. Rev.*, 2007, **107**, 2365.
12 C. Das Neves Gomes, O. Jacquet, C. Villiers, P. Thuéry, M. Ephritikhine and T. Cantat, *Angew. Chem., Int. Ed.*, 2012, **51**, 187.
13 (*a*) Y. Zhang, T. Zhang and S. Das, *Green Chem.*, 2020, **22**, 1800; (*b*) M. Hulla and P. J. Dyson, *Angew. Chem., Int. Ed.*, 2020, **59**, 1002; (*c*) R. A. Pramudita and K. Motokura, *Green Chem.*, 2018, **20**, 4834; (*d*) A. Tlili, E. Blondiaux, X. Frogneux and T. Cantat, *Green Chem.*, 2015, **17**, 157.
14 Q. Zhang, X.-T. Lin, N. Fukaya, T. Fujitani, K. Sato and J.-C. Choi, *Green Chem.*, 2020, **22**, 8414.
15 (*a*) J. A. do Nascimento Neto, C. C. da Silva, L. Ribeiro, G. A. Vasconcelos, B. G. Vaz, V. S. Ferreira, L. H. K. Queiroz Jr, L. J. Q. Maia, A. M. Sarottic and F. T. Martins, *New J. Chem.*, 2017, **41**, 12843; (*b*) E. B. Dianov, I. G. Pervova, E. A. Dvoskin and P. A. Slepukhin, *Russ. J. Gen. Chem.*, 2018, **88**, 843.
16 (*a*) R. B. Nielsen, K. O. Kongshaug and H. Fjellvåg, *J. Mater. Chem.*, 2008, **18**, 1002; (*b*) R. A. Taylor, H. A. Ellis, P. T. Maragh and N. A. S. White, *J. Mol. Struct.*, 2006, **787**, 113.
17 S. Das, D. Addis, K. Junge and M. Beller, *Chem. – Eur. J.*, 2011, **17**, 12186; S. Das, D. Addis, S. Zhou, K. Junge and M. Beller, *J. Am. Chem. Soc.*, 2010, **132**, 1770.
18 (*a*) H. Niu, L. Lu, R. Shi, C.-W. Chiang and A. Lei, *Chem. Commun.*, 2017, **53**, 1148; (*b*) O. Jacquet, X. Frogneux, C. Das Neves Gomes and T. Cantat, *Chem. Sci.*, 2013, **4**, 2127; (*c*) Y. Li, X. Fang, K. Junge and M. Beller, *Angew. Chem., Int. Ed.*, 2013, **52**, 9568.